ISSN 1746-7659, England, UK
Journal of Information and Computing Science
Vol. 5, No. 2, 2010, *pp*. 133-145

Multiwavelet Computed Radon-Based Ofdm Trasceiver Designed and Symulation under Different Channel Conditions

Dr. Abbas Hasan Kattoush [1, +], Dr. Waleed Ameen Mahmoud [2], Dr. Atif Mashagbah [1] and Eng. Ahed Ghodayyah [3]

[1] Head of EE Department, Tafila Technical University - Jordan
[2] Dean of Engineering College Al-Isra University - Jordan
[3] EE Department, Al Ahliyya Amman University, Jordan

(*Received September 24, 2009, accepted October 22, 2009*)

Abstract. Finite Radon Transform (FRAT) mapper computed in Fourier basis using fast Fourier transform (FFT) algorithm has the ability to increase orthogonality of sub-carriers, it is non sensitive to channel parameters variations, and has a small constellation energy compared with conventional FFT based orthogonal frequency division multiplexing (OFDM). It is also able to work as a good interleaver which significantly reduces the bit error rate (BER) performance of the OFDM system under severe channel conditions. In this paper the idea is developed towards increasing the orthogonality and increasing spectral efficiency of OFDM system structure. FRAT computed in discrete Multiwavelet transform (DMWT) basis is implemented in OFDM systems and compared with FRAT OFDM computed in Fourier basis under different channel conditions for different channels parameters values including multi-path gains vector, multi-path delay time vector, and maximum Doppler shift. As a result, the proposed structure gives a significant improvement in BER performance in Additive White Gaussian Noise (AWGN) channels, flat fading channels (FFC), and multi-path selective fading channels (SFC).

Keywords: Discrete Multi-Wavelet Transform; Finite Radon Transform; Critical sampling algorithm; FRAT-FFT OFDM Transceiver; FRAT-DMWT OFDM Transceiver.

1. Introduction

Orthogonal frequency division multiplexing system is one of the most promising technologies for current and future wireless communications. It is a form of multi-carrier modulation technologies where data bits are encoded to multiple sub-carriers, while being sent simultaneously [1]. The process of combining different sub-carriers to form a composite time-domain signal is achieved using FFT and inverse FFT (IFFT) operations [2].

The main problem in the design of a communications system over a wireless link is to deal with multi-path fading, which causes a significant degradation in terms of both the reliability of the link and the data rate [3]. Multi-path fading channels have a severe effect on the performance of wireless communication systems even those systems that exhibits efficient bandwidth, like OFDM [4]. There is always a need for developments in the realization of these systems as well as efficient channel estimation and equalization methods to enable these systems to reach their maximum performance [5]. The OFDM receiver structure allows relatively straightforward signal processing to combat channel delay spreads, which was a prime motivation to use OFDM modulation methods in several standards.

The conventional Fourier based OFDM uses the complex exponential bases functions. Later these functions were replaced by orthonormal wavelets in order to reduce the level of interference as in references [6-9]. It was found that the Haar-based orthonormal wavelets are capable of reducing inter symbol interference (ISI) and inter carrier interference (ICI), which are caused by the loss in orthogonality between the carriers [6]. A main motivation for using wavelet-based OFDM is the superior spectral containment properties of wavelet filters over Fourier filters. It has been found that under certain channel conditions,

[+] Corresponding author. *E-mail address*: akattoush@yahoo.ca

Wavelet OFDM does outperform Fourier OFDM and under other channel conditions the situation is reversed as in the selective fading channels. Further performance gains can be made by looking at alternative orthogonal basis functions and found a better transform rather than Fourier and wavelet transform.

The Radon transform (RT) was first introduced by Johann Radon (1917) and the theory, basic aspects, and applications of this transform are studied in [10-12] while the FRAT was first studied by [13]. RT is the underlying fundamental concept used for computerized tomography scanning, as well for a wide range of other disciplines, including radar imaging, geophysical imaging, nondestructive testing and medical imaging [10]. Recently FRAT was proposed as a mapping technique in OFDM system [14]. As a result of applying FRAT, the BER performance was improved significantly, especially in the existence of multi-path fading channels. Also, it was found that Radon-based OFDM structure is less sensitive to channel parameters variation as compared with standard OFDM structure.

In this paper the idea of one dimensional serial Radon based OFDM proposed in [14] is develop farther to words increasing spectral efficiency and reducing BER. FFT and IFFF in FRAT computation algorithm are replaced by DMWT and inverse DMWT (IDMWT). The new Radon-DMWT based OFDM system is based on a fast computation method for DMWT, the critical sampling algorithm. The purpose of this multiplicity is to achieve more properties which can not be combined in other transforms (Fourier and wavelet) [15]. Simulation results show that proposed system has better performance than Fourier, Radon, and wavelet based OFDM under different channel conditions.

2. Discrete Multiwavelet Transform Computation

As a natural extension of wavelet, Multiwavelet are designed to be simultaneously symmetric, orthogonal and having short supports with high approximation power, which cannot be achieved at the same time for wavelet using only one scaling function. The trick is to increase the number of scaling functions to raise the approximation power rather than one scaling function. It enhances the performance of many wavelet applications such as image coding and de-noising [16-17].

In particular, whereas wavelets have an associated scaling function $\phi(t)$ and wavelet function $\Psi(t)$, multiwavelets have two or more scaling and wavelet functions. For notational convenience, the set of scaling functions can be written using the vector notation $\Phi(t) \equiv [\phi_1(t), \phi_2(t) \cdots \phi_r(t)]^T$, where $\Phi(t)$ is called the multi-scaling function. Likewise, the multiwavelet function is defined from the set of wavelet functions as $\Psi(t) \equiv [\psi_1(t), \psi_2(t) \cdots \psi_r(t)]^T$. When $r=1$, $\Psi(t)$ is called a scalar wavelet, or simply wavelet. While in principle r can be arbitrarily large. The multiwavelets studied to date are primarily for $r=2$ [18].

The multiwavelet two-scale equations resemble those for scalar wavelets [19]:

$$\Phi(t) = \sqrt{2} \sum_{k=-\infty}^{\infty} H_k \Phi(2t-k) \tag{1}$$

$$\Psi(t) = \sqrt{2} \sum_{k=-\infty}^{\infty} G_k \Phi(2t-k) \tag{2}$$

Note, however, that $\{H_k\}$ and $\{G_k\}$ are matrix filters, i.e., H_k and G_k are $(r \times r)$ matrices for each integer k. The matrix elements in these filters provide more degrees of freedom than a traditional scalar wavelet. These extra degrees of freedom can be used to incorporate useful properties into the multiwavelet filters, such as orthogonality, symmetry, and high order of approximation. However, the multi-channel nature of multiwavelets also means that the sub-band structure resulting from passing a signal through a multi-filter bank is different [18].

The two-scale equations (1) and (2) can be realized as a matrix filter bank operating on *r* input data stream and filtering them into *2r* output data streams, each of which is down-sampled by a factor two.

One famous multiwavelet filter is proposed by Geronimo, Hardian, and Massopust (GHM), the GHM filter [20]. The GHM basis offers a combination of orthogonality, symmetry, and compact support, which can not be achieved by any scalar wavelet basis [21]. According to equations (1) and (2) for GHM system H_k are four scaling matrices H_0, H_1, H_2, and H_3, and G_k are four wavelet matrices G_0, G_1, G_2, and G_3 [22].

$$H_0=\begin{bmatrix}\frac{3}{5\sqrt{2}} & \frac{4}{5}\\ -\frac{1}{20} & -\frac{3}{10\sqrt{2}}\end{bmatrix},\ H_1=\begin{bmatrix}\frac{3}{5\sqrt{2}} & 0\\ \frac{9}{20} & \frac{1}{\sqrt{2}}\end{bmatrix},\ H_2=\begin{bmatrix}0 & 0\\ \frac{9}{20} & -\frac{3}{10\sqrt{2}}\end{bmatrix},\ H_3=\begin{bmatrix}0 & 0\\ -\frac{1}{20} & 0\end{bmatrix} \tag{3}$$

$$G_0=\begin{bmatrix}-\frac{1}{20} & -\frac{3}{10\sqrt{2}}\\ \frac{1}{10\sqrt{2}} & \frac{3}{10}\end{bmatrix},\ G_1=\begin{bmatrix}\frac{9}{20} & -\frac{1}{\sqrt{2}}\\ -\frac{9}{10\sqrt{2}} & 0\end{bmatrix},\ G_2=\begin{bmatrix}\frac{9}{20} & -\frac{3}{10\sqrt{2}}\\ \frac{9}{10\sqrt{2}} & -\frac{3}{10}\end{bmatrix},\ G_3=\begin{bmatrix}-\frac{1}{20} & 0\\ -\frac{1}{10\sqrt{2}} & 0\end{bmatrix} \tag{4}$$

The multiwavelet coefficients that the low-pass filter (LPF) H and high-pass filter (HPF) G consists of are $r\times r$ matrices, and during the convolution step they must multiply vectors (instead of scalars). This means that multi-filter banks need r input rows. In this case $r=2$ and two data streams enter the multi-filter. To create the two data streams from an ordinary single-stream input of length N, there are several possibilities. An important one of them is to create consistent approximation based equations that yield two length $N/2$ streams and a "de-approximation" that returns a length N stream. This method maintains a critically sampled representation (produces $N/2$ length-2 vectors). The multi-filter processes two $N/2$ point data streams using an approximation method suggested by Geronimo [20].

The aim of preprocessing is to associate the given scalar input signal of length N (must be a power of 2) to a sequence of length-2 vectors in order to start the analysis algorithm. After the wavelet transform, inverse transform, and post-filtering should recover the input signal exactly if nothing else has been done. For critically sampled multiwavelets there are two methods of approximation: First-order approximation method and second- order approximation method.

The first order approximation-based preprocessing [21] (where every two rows generate two new rows) can be summarized as follows:

- For any odd row

$$\begin{aligned}new\ odd\text{-}row = {} & (0.373615)[same\ odd\text{-}row] +\\ & (0.11086198)[next\ even\text{-}row] +\\ & (0.11086198)[previous\ even\text{-}row]\end{aligned} \tag{5}$$

- For any even-row

$$new\ even\text{-}row = (\sqrt{2}-1)[same\ even\text{-}row] \tag{6}$$

The second order approximation-based preprocessing [21] (where every two rows generate two new rows) can be summarized as follows:

– For any odd row

$$\begin{aligned}new\ odd\text{-}row = {} & (10/8\sqrt{2})[same\ odd\text{-}row] +\\ & (3/8\sqrt{8})[next\ even\text{-}row] +\\ & (3/8\sqrt{2})[previous\ even\text{-}row]\end{aligned} \tag{7}$$

– For any even-row

$$new\ even\text{-}row = [same\ even\text{-}row] \tag{8}$$

It should be noted that when computing the first odd row, the previous even-row in equation (5) is equal to zero. The same thing is valid for equation (7).

For computing DMWT, scalar wavelet transform matrices can be written as follows:

$$W=\begin{bmatrix} H_0 & H_1 & H_2 & H_3 & 0 & 0 & \cdots & 0 & 0 & 0 & 0 \\ 0 & 0 & H_0 & H_1 & H_2 & H_3 & \cdots & 0 & 0 & 0 & 0 \\ \vdots & \vdots & \vdots & \vdots & \vdots & \vdots & \cdots & \vdots & \vdots & \vdots & \vdots \\ H_2 & H_3 & 0 & 0 & 0 & 0 & \cdots & 0 & 0 & H_0 & H_1 \\ G_0 & G_1 & G_2 & G_3 & \vdots & \vdots & \cdots & 0 & 0 & 0 & 0 \\ 0 & 0 & G_0 & G_1 & G_2 & G_3 & \cdots & 0 & 0 & 0 & 0 \\ \vdots & \vdots & \vdots & \vdots & \vdots & \vdots & \cdots & \vdots & \vdots & \vdots & \vdots \\ 0 & 0 & 0 & 0 & 0 & 0 & \cdots & G_0 & G_1 & G_2 & G_3 \\ G_2 & G_3 & 0 & 0 & 0 & 0 & \cdots & 0 & 0 & G_0 & G_1 \end{bmatrix} \quad (9)$$

where H_i and G_i are the low and HPF impulse responses, which are 2×2 matrices.

By examining the transform matrices of the scalar wavelet equations and multiwavelets equation (9), one can see that in the multiwavelet transform domain there are first and second HPF coefficients rather than one low-pass coefficient followed by one high-pass coefficient. Therefore, if these four coefficients are separated, there are four sub-bands in the transform domain.

Fast DMWT computation for 1-D signal using critically sampling is computed using the following procedure:

- Checking input dimensions: Input vector should be of length N, where N must be power of two.
- Constructing a $N/2\times N/2$ transformation matrix W using GHM low and HPFs matrices given in equations (3) and (4) respectively. After substituting GHM matrix filter coefficients values, an $N\times N$ transformation matrix results
- Preprocessing rows: Approximation-based row preprocessing can be computed by applying equations (5) and (6) to the odd and even-rows respectively of the input $N\times N$ matrix for the first order approximation preprocessing. For the second order approximation preprocessing, equations (5) and (6) are used for preprocessing odd and even-rows of the input $N\times 1$ matrix P respectively.
- Transformation of input vector which can be done by applying matrix multiplication to the $N/2\times N/2$ constructed transformation matrix by the $N\times 1$ preprocessing input vector. Transformation of input vector can be done as follows:
  $[Z]=[W]\times[P]^T$

The inverse of the upper procedure for computing inverse fast DMWT for 1-D signal using critically sampling algorithm is as follows:

- Let *X* be the $N\times 1$ multiwavelet transformed vector, where N is power of 2.
- Construct $N/2\times N/2$ reconstruction matrix $W_2=W^T$.
- Multiply a $N/2\times N/2$ reconstruction matrix W_2 with the $N\times 1$ multiwavelet transformed vector.
- Apply post-processing by using the following:
  - Compute post-processing first order approximation by:
    $$\text{odd - row}=[[\text{same odd - row}]-(0.11086198)[\text{next even - row}]-(0.11086198)[\text{previous even - row}]]/(0.373615)$$
    $$\text{even - row}=[\text{same even - row}]/(\sqrt{2}-1)$$
    to the column reconstructed $N\times 1$ vector matrix.
  - Compute post-processing second order approximation by applying equations:
    $$\text{odd - row}=[[\text{same odd - row}]-(3/8\sqrt{8})[\text{next even - row}]-(3/8\sqrt{2})[\text{previous even - row}]]/(10/8\sqrt{2})$$
    $$\text{even - row}=[\text{same even - row}]$$
    to the column reconstructed $N\times 1$ vector matrix P.

Reconstruction of input transformation vector can be done as follows: $[z]=[W_2]\times[p]^T$

3. The Radon-based OFDM

Radon-based OFDM was recently proposed in [14], it was found that as a result of applying FRAT, the BER performance was improved significantly, especially in the existence of multi-path fading channels. Also, it is found that Radon-based OFDM structure is less sensitive to channel parameters variation, like maximum delay, path gain, and maximum Doppler shift in selective fading channels as compared with standard OFDM structure.

In radon based OFDM system, FRAT mapping is used instead of quadrature amplitude modulation (QAM) mapping [14] as shown in Fig. 1. The other processing parts of the system remain the same as in conventional QAM OFDM system. It is known that fast Fourier transform based OFDM obtain the required orthogonality between sub-carriers from the suitability of IFFT algorithm [2, 4, 13]. Using FRAT mapping with the OFDM structure increases the orthogonality between sub-carriers since FRAT computation uses one-dimensional (1-D) IFFT algorithm. Also FRAT is designed to increase the spectral efficiency of the OFDM system through increasing the bit per Hertz of the mapping. Sub carriers are generated using N points discrete Fourier transform (DFT) and guard interval (GI) inserted at start of each symbol is used to reduce ISI.

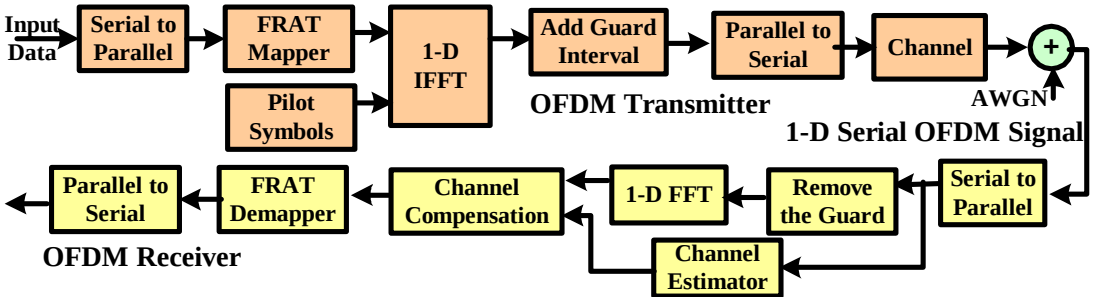

Fig. 1: Serial Radon based OFDM transceiver.

The procedure steps of using the Radon based OFDM mapping is as follows:

Step 1: Suppose $d(k)$ is the serial data stream to be transmitted using OFDM modulation scheme. Converting $d(k)$ from serial form to parallel form will construct a one dimensional vector containing the data symbols to be transmitted,

$$d(k) = \left(d_0\ d_1\ d_2\ .....\ d_n\right)^T \tag{10}$$

Where, k and n are the time index and the vector length respectively.

Step 2: convert the data packet represented by the vector $d(k)$ from one-dimensional vector to a $p \times p$ two dimensional matrix $D(k)$, where p should be a prime number according to the matrix resize operation.

Step 3: Take the 2-dimensional (2-D) FFT of the matrix $D(k)$ to obtain the matrix, $F(r,s)$. For simplicity it will be labeled by F.

$$F(r,s) = \sum_{m=0}^{p-1}\sum_{n=0}^{p-1} D(m,n) e^{-j(2\pi/p)rm} e^{-j(2\pi/p)ns} \tag{11}$$

Step 4: Redistribute the elements of the matrix F according to the optimum ordering algorithm given in [23]. So, the dimensions of the resultant matrix will be $p \times (p+1)$ and will be denoted by the symbol F_{opt}. The two matrixes for FRAT window= 7 are given by:

$$\mathsf{F} = \begin{bmatrix} f_1 & f_8 & f_{15} & f_{22} & f_{29} & f_{36} & f_{43} \\ f_2 & f_9 & f_{16} & f_{23} & f_{30} & f_{37} & f_{44} \\ f_3 & f_{10} & f_{17} & f_{24} & f_{31} & f_{38} & f_{45} \\ f_4 & f_{11} & f_{18} & f_{25} & f_{32} & f_{39} & f_{46} \\ f_5 & f_{12} & f_{19} & f_{26} & f_{33} & f_{40} & f_{47} \\ f_6 & f_{13} & f_{20} & f_{27} & f_{34} & f_{41} & f_{48} \\ f_7 & f_{14} & f_{21} & f_{28} & f_{35} & f_{42} & f_{49} \end{bmatrix} \tag{12}$$

$$\mathsf{F}_{\text{opt}} = \begin{bmatrix} f_1 & f_1 & f_1 & f_1 & f_1 & f_1 & f_1 & f_1 \\ f_2 & f_{10} & f_9 & f_{16} & f_8 & f_{21} & f_{14} & f_{13} \\ f_3 & f_{19} & f_{17} & f_{31} & f_{15} & f_{34} & f_{20} & f_{18} \\ f_4 & f_{28} & f_{25} & f_{46} & f_{22} & f_{47} & f_{26} & f_{23} \\ f_5 & f_{30} & f_{33} & f_{12} & f_{29} & f_{11} & f_{32} & f_{35} \\ f_6 & f_{39} & f_{41} & f_{27} & f_{36} & f_{24} & f_{38} & f_{40} \\ f_7 & f_{48} & f_{49} & f_{42} & f_{43} & f_{37} & f_{44} & f_{45} \end{bmatrix} \tag{13}$$

Step 5: Take the 1D-IFFT for each column of the matrix F_{opt} to obtain the matrix of Radon coefficients, R:

$$R = \frac{1}{p} \sum_{k=0}^{N-1} F_{opt}\, e^{\frac{j 2 \pi k n}{p}} \tag{14}$$

Step 6: Construct the complex matrix $\overline{R}$ from the real matrix R such that its dimensions will be $p \times (p+1)/2$ according to:

$$\overline{r_{l,m}} = r_{i,j} + j \quad r_{i,j+1}, 0 \le i \le p, 0 \le j \le p \tag{15}$$

Where, $\overline{r_{l,m}}$ refers to the elements of the matrix $\overline{R}$, while $r_{i,j}$ refers to the elements of the matrix R. Matrixes R and $\overline{R}$ are given by:

$$\mathsf{R} = \begin{bmatrix} r_{1,1} & r_{1,2} & r_{1,3} \cdots\cdots & r_{1,p+1} \\ r_{2,1} & r_{2,2} & r_{2,3} \cdots\cdots & r_{2,p+1} \\ \vdots & \vdots & \vdots \quad \cdots\cdots & \vdots \\ \vdots & \vdots & \vdots \quad \cdots\cdots & \vdots \\ r_{p-1,1} & r_{p-1,2} & \cdots\cdots & r_{p-1,p+1} \\ r_{p,1} & r_{p,2} & r_{p,3} \cdots\cdots & r_{p,p+1} \end{bmatrix} \tag{16}$$

$$\overline{\mathsf{R}} = \begin{bmatrix} r_{1,1} + jr_{1,2} & r_{1,3} + jr_{1,4} \cdots\cdots & r_{1,p} + jr_{1,p+1} \\ r_{2,1} + jr_{2,2} & r_{2,3} + jr_{2,4} \cdots\cdots & r_{2,p} + jr_{2,p+1} \\ \vdots \quad \vdots & \vdots \quad \cdots\cdots & \vdots \quad \vdots \\ \vdots \quad \vdots & \vdots \quad \cdots\cdots & \vdots \quad \vdots \\ r_{p-1,1} + jr_{p-1,2} & \cdots\cdots & r_{p-1,p} + jr_{p-1,p+1} \\ r_{p,1} + jr_{p,2} & \cdots\cdots & r_{p,p} + jr_{p,p+1} \end{bmatrix} \tag{17}$$

Complex matrix construction is made for a purpose of increasing bit per Hertz of mapping before resizing mapped data.

Step 7: Resize the matrix $\overline{R}$ to a one dimensional vector $r(k)$ of length $p \times (p+1)/2$.

$$r(k) = \left(r_0\ r_1\ r_2\ \ldots\ldots\ r_{p(p+1)/2}\right)^T \tag{18}$$

Step 8: Take the 1D-IFFT for the vector, $r(k)$ to obtain the sub-channel modulation.

$$s(k) = \frac{1}{p(p+1)/2} \sum_{k=0}^{N_C - 1} r(k) e^{\frac{j 2 \pi k n}{p(p+1)/2}} \quad \ldots (19)$$

where N_C number of carriers.

Step 9: Finally, convert the vector $s(k)$ to serial data symbols: $s_0,\ s_1,\ s_2,\ \ldots\ldots,\ s_n$.

4. Proposed FRAT-OFDM System computed in DMWT- basis

The procedure that realizes the steps of FRAT is illustrated in Fig. 2 and the block diagram of proposed

system is shown in Fig. 3. It represents a signal flow diagram that explains the proposed OFDM transmitter. At the start the input data streams are converted from serial to parallel so as to construct a one dimensional vector that contains the data symbols to be transmitted as given by equation (20)

$$d = (d_1\ d_2\ .....\ d_{N^2})^T \tag{20}$$

where, N^2 is the specified frame length, and N should be power of 2.

Then the data packets which are represented by the vector d are converted from one-dimensional vector to an $N \times N$ 2-dimensional matrix D, according to the matrix resize operation. The FRAT operation is performed on the matrix D to obtain the matrix R of dimensions $2N \times p+1$. The first step in computing the FRAT using DMWT is the computation of the 2-D DMWT of the matrix D using discrete Multiwavelets Critically-Sampled (DMWTCS). The output matrix will be resized to dimensions $p \times p$ by adding zeros to rows and columns, where p is the smallest prime number after N. Optimum ordering is taken over the prime matrix to perform optimum ordering matrix of dimensions $p \times p+1$. Then the optimum ordered matrix is resized by adding zeros to the columns to make its dimension $2N \times p+1$. The zeros added are like the zeros padded in the OFDM system, and after this step the 1-D DMWT is computed. The modifications made on data dimensions at the end of calculating the FRAT matrix coefficients R, are for the purpose of increasing the bit per Hertz of the mapping before resizing the mapped data. And it is achieved by constructing the complex matrix $\overline{R}$ from the real matrix R such that its dimensions become $2N \times (p+1)/2$ according to:

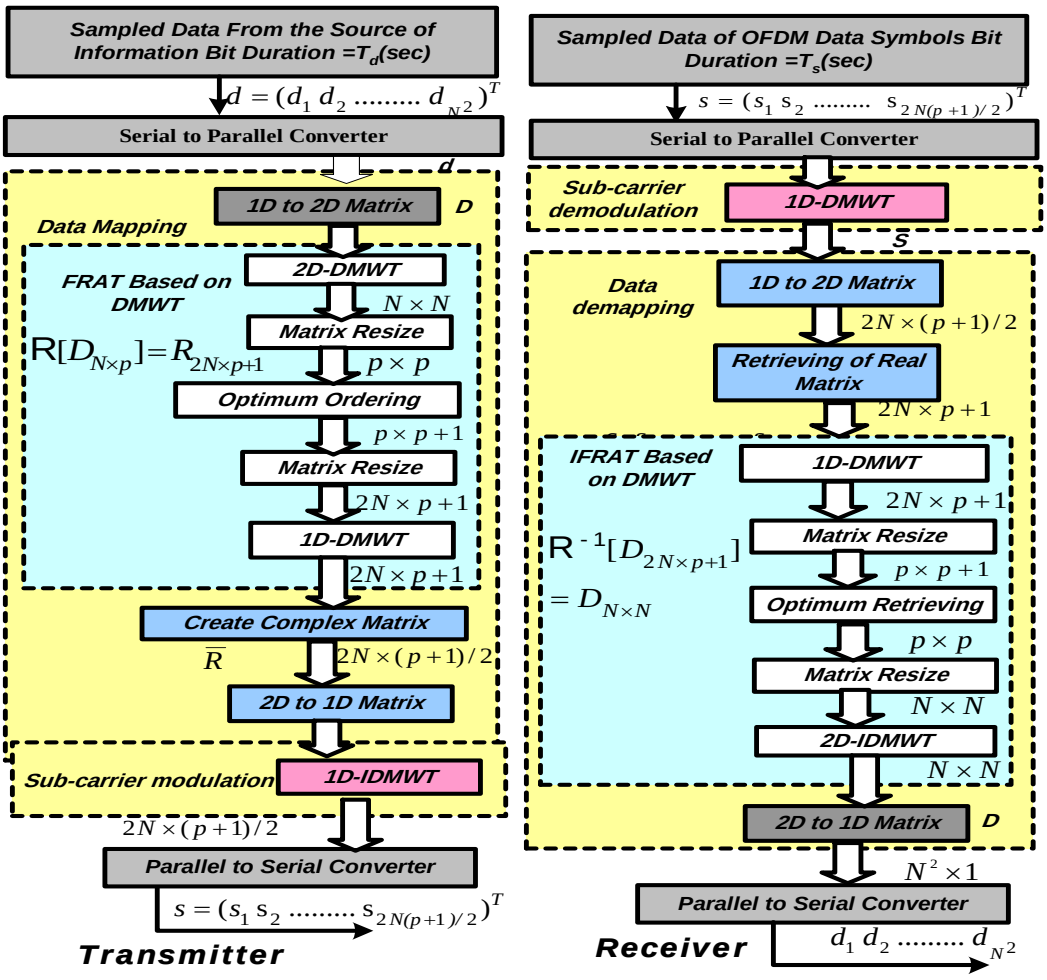

Fig. 2: The flow diagram of the proposed FRAT-OFDM transceiver realized in DMWT- basis.

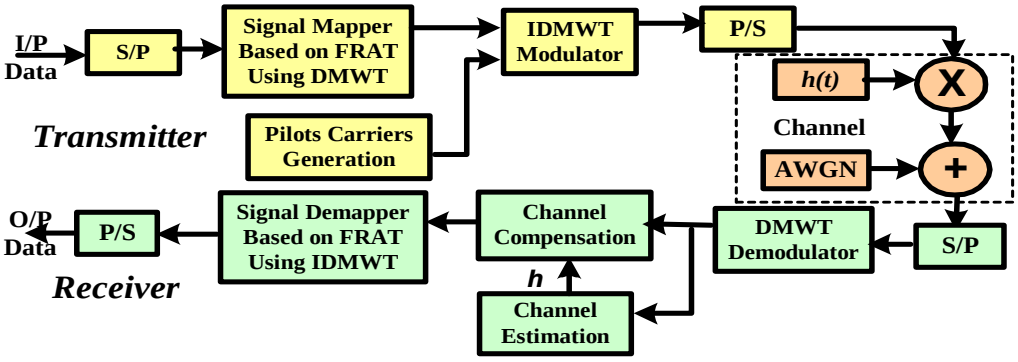

Fig. 3: Block Diagram of Proposed OFDM System Based on DMWT-bases FRAT

$$\bar{r}_{l,m} = r_{i,j} + i \times r_{i,j+1},\ 1 \le i \le 2N,\ 1 \le j \le p+1 \tag{21}$$

where, $\bar{r}_{l,m}$, refers to the elements of the matrix $\bar{R}$, while $r_{i,j}$ refers to the elements of the matrix R.

Finally mapping is done by resizing the matrix to a 1-D vector r of length $2N \times (p+1)/2$ as in equation (22).

$$r = (r_1\ r_2\ .....\ r_{2N(p+1)/2})^T \tag{22}$$

And the complex valued symbols are now ready for sub-carrier modulation.

After the FRAT based on DMWT has been done, a pilot-carrier (training sequence) is generated which is a bipolar sequence {±1}.The receiver will be informed about this sequence previously and the training sequence is inserted in parallel with data. The two sequences (data plus training) are transformed by 1-D IDMWT to have the vector r in order to obtain the sub-channel modulation.

Finally, the two sequences (training plus data) are converted to one sequence using P/S converter which converts the vector s to serial data symbols $s_1\ s_2\ .....\ s_{2N(p+1)/2}$

It is important here to point out that data mapper achieved in the conventional FFT-based OFDM by quadrature phase shift keying and QAM modulations is replaced by the FRAT to get the constellated data prior to the sub-channel modulation.

The receiver procedure is the reversed procedure of the transmitter and from it, it can be seen how the data dimensions are changing throughout the blocks. At the receiver, S/P converts the received sequence to a parallel form then passes the packet to 1-D DMWT. After the zeros pad are removed, the signal represents data plus training. The training sequence is used to estimate the channel frequency response as follows:

$$H(k) = \frac{\text{Re}\,ceived\ Training\ Samples\,(k)}{Transmitted\ Training\ Samples\,(k)},\ k = 1,2,...,N \tag{23}$$

The channel frequency response is used to compensate the channel effects on the data, and the estimated data can be found using equation (24):

$$Estimate\,\text{Data}\,(k) = H^{-1}_{Estimate}(k) \times \text{Re}\,ceived\ \text{Data}\,(k),\ k = 1,2,...,2N \times (p+1)/2 \tag{24}$$

The output of channel compensator is passed through the signal demapper based on inverse FRAT. Finally P/S converts the parallel data serial.

5. Performance of FRAT based OFDM Transceiver

In following sections FRAT-based OFDM transceiver is simulated, and its performance is analyzed. System parameters used through the simulation are $T_d = 0.1\mu\text{sec}$, FRAT window 8×8, DMWTCS bins= 64, Guard interval is a Cyclic prefix approach with 26 symbols added to the frame, and Pilot-assisted channel estimator. The output of FRAT is (16×6), so the frame of sub carrier modulation is of length 64×2 after the training is inserted into to the frame and before sending it through the channel. Different types of channel models are taken into account during the simulation. AWGN channel is considered with several SNR values. Then multi-path Raleigh distributed fading channels are considered with two scenarios: flat and multi-path selective fading cases. Fig. 3 is the schematic block diagram used for the proposed OFDM transceiver

simulations. The pilot-assisted channel estimator is used here to combat the channel fading effects since it is an efficient method especially for the case of slow fading channels.

5.1. The FRAT based OFDM in AWGN Environment

A MATLAB 7.0 was used to simulate the proposed FRAT-based OFDM transceiver shown in Fig. 3. The simulation results of proposed FRAT-OFDM system in AWGN channel are shown in Fig. 4. From which it is clearly seen that DMWTCS based FRAT-OFDM has much better performance than FFT based FRAT-OFDM. This reflects the fact that the orthogonality of Multiwavelets based FRAT-OFDM is much higher than the orthogonality of FFT-OFDM.

5.2. The FRAT-OFDM in Flat fading channel

The same programs used for simulations in AWGN channel are used here to simulate the results in a flat fading channel with AWGN. In this case all frequency components in the signal are affected by a constant attenuation and a linear phase distortion of the channel, which has been chosen to have a Rayleigh's distribution. A Doppler frequency of 10 Hz is used in this simulation and the results of simulations are provided in Fig .5. It can be seen from Fig 5 that FRAT-OFDM using DMWTCS outperforms significantly the other system for this channel model.

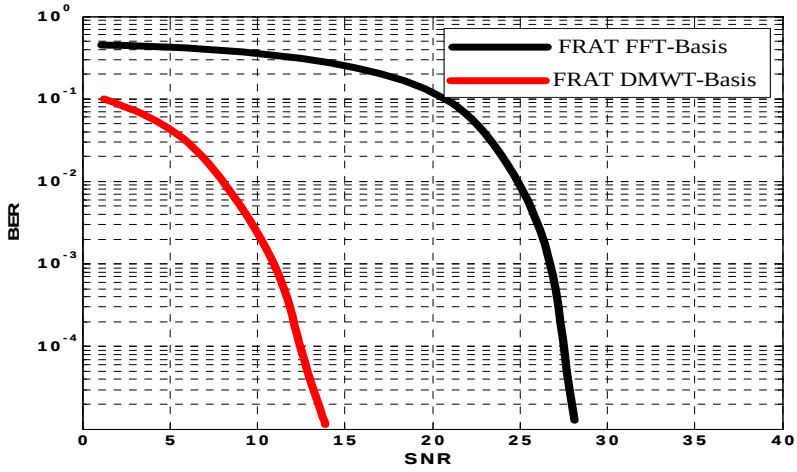

Fig. 4: BER performance of FRAT-OFDM using DMWTCS and FFT in AWGN channel model

Alternative Doppler shift frequencies are used; the values taken are 100Hz, and 500Hz. The BER performance verses SNR are given in Fig. 6 and Fig. 7.

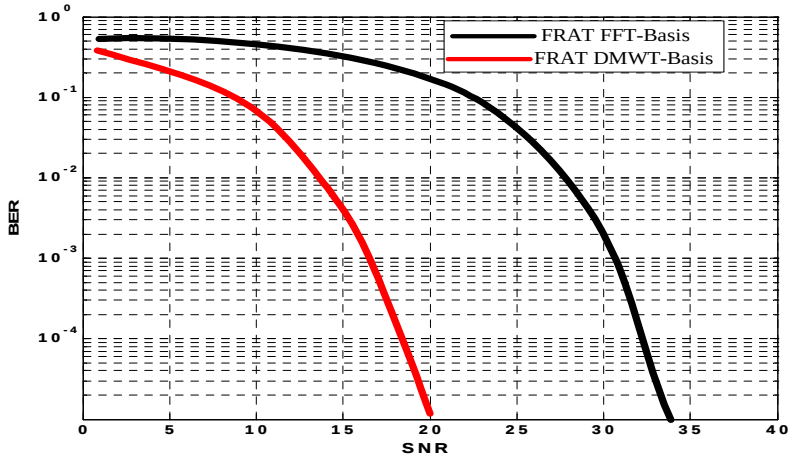

Fig. 5: BER performance of FRAT-OFDM using DMWTCS and FFT in FFC at Max Doppler Shift =10Hz

5.3. The FRAT-OFDM in Frequency Selective fading channel

In this section, BER performance of FRAT-OFDM using DMWTCS and FFT are simulated in a multi-path frequency selective Rayleigh distributed channels with AWGN. Two rays channel is assumed here with

a second path gain of -8dB at a maximum delay from the second path of τ_{max}=0.1μsec for several values of SNR.

Fig. 8 shows simulations at maximum Doppler shift, $f_{D\max} = 10Hz$, a symbol time $T_d = 0.1\mu\text{sec}$, a maximum delay in the second path $\tau_{\max} = 0.1\mu\text{sec}$. The same simulations are repeated and shown in Fig. 9 and Fig. 10 for $f_{D\max} = 100Hz$ and 500Hz respectively. All other parameters are kept the same as in the previous cases. It is clearly seen from figures that the performance of DMWTCS FRAT-OFDM is superior to that of FFT based FRAT-OFDM system.

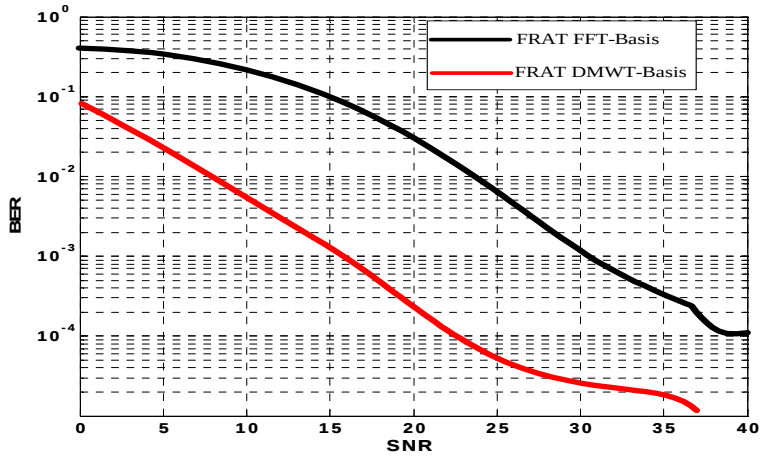

Fig. 6: The BER performance of FRAT-OFDM using DMWTCS and FFT in FFC at Max. Doppler Shift=100Hz.

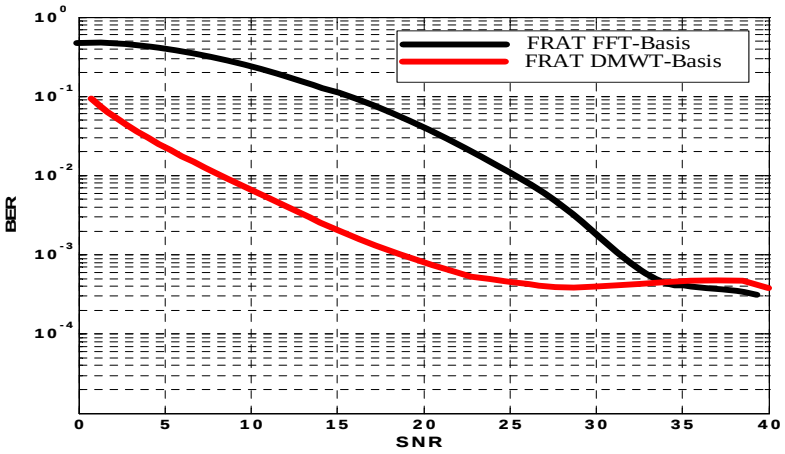

Fig. 7: BER performance of FRAT-OFDM using DMWTCS and FFT in FFC at Max. Doppler Shift=500Hz.

6. Conclusions

In this paper, the FRAT method for data mapping in OFDM system is developed and implemented, FRAT is computed in DMWTCS basis instead of FFT basis and the suitability for such implementation was verified by simulations. In AWGN, flat fading channel and selective fading channel the Multiwavelet based FRAT OFDM outperform the other OFDM system and offers a large improvement in SNR. As a result of applying the DMWTCS-FRAT the BER performance was improved significantly especially in the multi-path fading channels. Also it can be concluded that the DMWTCS-FRAT OFDM is less sensitive to channel parameters variations like maximum Doppler shift in selective fading channels as compared with the standard OFDM structure. Therefore, this structure can be considered as an alternative to the conventional OFDM.

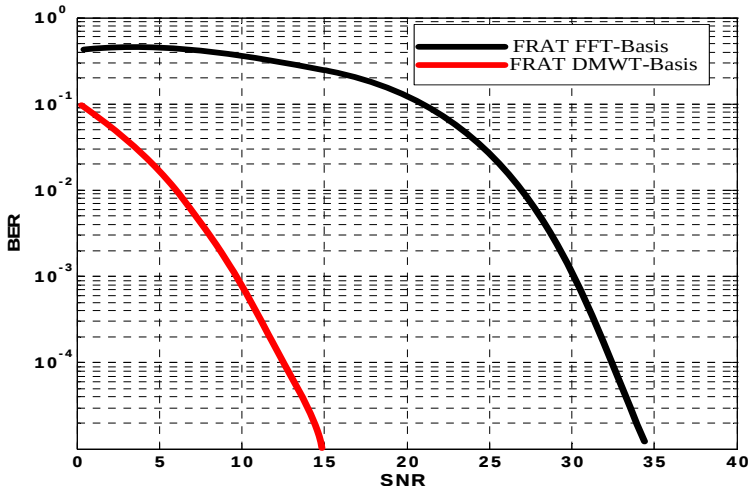

Fig. 8: The BER performance of FRAT-OFDM using DMWTCS and FFT in Selective Fading Channel at Max Doppler Shift=10Hz.

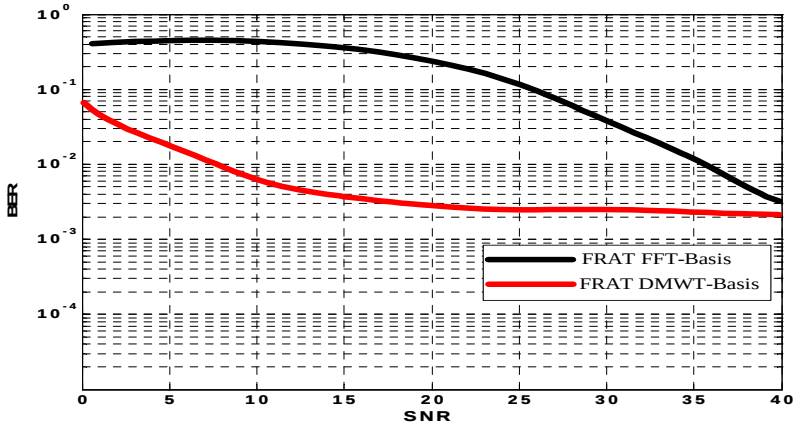

Fig. 9: The BER performance of FRAT-OFDM using DMWTCS and FFT in SFC at Max Doppler Shift=100Hz.

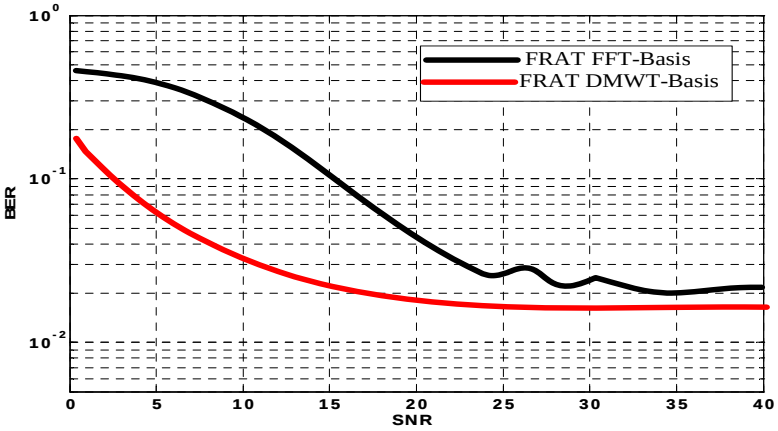

Fig. 10: The BER performance of FRAT-OFDM using DMWTCS and FFT in SFC at Max Doppler Shift=500Hz.

7. References

[1] N. Al-Dhahir and J.M. Cioffi. Optimum finite-length equalization for multicarrier transceivers. *IEEE Trans. Communications.* 1996, **44**(1): 56-64.

[2] S. Weinstein and P. Ebert. Data Transmission by Frequency Division Multiplexing using the Discrete Fourier Transform. *IEEE Trans. Commun. Tech.* 1971, **COM-19**(10): 628-634.

[3] Nghi H. Tran, Ha H. Nguyen, and Tho Le-Ngoc. Bit-Interleaved Coded OFDM With Signal Space Diversity:

Subcarrier Grouping and Rotation Matrix Design. *IEEE Transactions On Signal Processing.* 2007, **55**(3): 1137-1149.

[4] E. Lawrey. *The Suitability of OFDM as a Modulation Technique for Wireless Telecommunications, with a CDMA Comparison, Thesis*. James Cook University, Oct. 1997.

[5] Won Gi Jeon, Kyung Hi Chang and Yong Soo Cho. An Equalization Technique for Orthogonal Frequency-Division Multiplexing Systems in Time-Variant Multipath Channels. *IEEE Transactions On Communications.* 1999, **47** (1): 27-32.

[6] S. Mallat. *A Wavelet Tour of Signal Processing, second ed*. New York: Academic Press, 1999.

[7] A.R. Lindsey. Wavelet packet modulation for orthogonally multiplexed communication. *IEEE Trans. Signal Process*. 1997, **45**: 1336-1337.

[8] X. Zhang, P. Xu, G. Zhang, G. Bi. Study on complex wavelet packet based OFDM modulation (CWP-OFDM). *ACTA Electron, Sinica.* 2002, **30**: 476–479.

[9] H. Zhang, D. Yuan, M. Jiang, D. Wu. Research of DFT-OFDM and DWT-OFDM on different transmission scenarios. *IEEE ICITA'2004.* Harbin, China, 2004. January 8-11.

[10] S. R. Deans. *The Radon transform and some of its applications.* New York: John Wiley & Sons, 1983.

[11] E. D. Bolker. The Finite radon transform. *Integral Geometry, Contemporary Mathematics.* 1987, **63**: 27-50.

[12] F. Natterer. *The mathematics of computerized tomography.* John Wiley & Sons, 1989.

[13] G. Beylkin. Discrete Radon transforms. *IEEE Trans. Acoustic, Speech and Signal Processing.* 1987, **ASSP-35**: 162-172.

[14] W. Al-Jawhar, Abbas H. Kattoush, S. M. Abbas, A. T. Shaheen. A High Speed High performance Parallel Radon Based OFDM Transceiver Design and Simulation. *Elsevier, Digital Signal Processing*. 2008, **18**: 907–918.

[15] M. Cotronei, L. B. Montefusco and L. Puccio. Multiwavelet Analysis and Signal Processing. *IEEE Trans. on Circuits and System-II.* 1998 August , **45**(8): 970-987.

[16] T. Hsung, Y. H. Shum and D. P. K. Lun. Orthogonal Symmetric Prefilter Banks for Discrete Multiwavelet Transforms. *Proceedings of International Symposium on Intelligent Signal Processing and Communication Systems.* Hong Kong: 2005, December 13-16.

[17] L. Wang, J. Lu, Y. Li, and T. Yahagi. Multiwavelet-Domain Filtering for Degraded Images with Gaussian Noise. *Graduate School of Science and Technology, Chiba University*. Japan, Industrial Technology, IEEE International Conference. 2005 Dec.14-17, pp.28-32.

[18] H. Wang, J. WANG, and W. WANG. Multispectral Image Fusion Approach Based on GHM Multiwavelet Transform. *Proceedings of the Fourth International Conference on Machine Learning and Cybernetics.* Guangzhou: 2005 August 18-21 © IEEE.

[19] Martin M. B. and Bell A. E. New Image Compression Techniques Using Multiwavelets and Multiwavelet Packets. *IEEE Transactions on Image Processing.* 2001 April, **10**(4).

[20] J. Geronimo, D. Hardin, and P.R. Massupost. Fractal Function and Wavelet Expansions Based on Several Functions. *J. Approx. Theory.* 1994, **78**: pp.373-401.

[21] Z. J. Mohammed. *VIDEO Image Compression based on Multiwavelets Transform.* Ph.D Thesis, University of Baghdad, 2004.

[22] V. Strela, and A. T. Walden. Orthogonal and Biorthogonal Multiwavelets for Signal Denoising and Image Compression. *Proc. SPIE.* 1998, **3391**:96-107.

[23] Minh N. Do and Martin Vetterli. The finite ridgelet transform for image representation. *IEEE Trans. Image Processing.* 2003 Jan., **12**(1): 16-28.

Abbas Hasan Kattoush received his M.S., and Ph.D. degrees in communication Eng. from USSR in 1979 and 1984 respectively. For 10 years Dr Kattoush was a technical manager of a leading SAKHER computers company. He was a pioneer in computer networking and software engineering in Jordan. From 1993 to 2000 he worked at Applied Science University Amman Jordan where he was a founding member and a head of the department of electrical and computer engineering. In 2000 Dr. Kattoush moved to Al-Isra University, Amman-Jordan where he worked as an associate professor and a head of department of Electrical and Computer Engineering until October 2008. Currently he is an associate professor and a head of department of Electrical and Computer Engineering at Tafila Technical University, Tafila-Jordan. His areas of research interest include DSP, digital communication systems, phase unwrapping, interferometric SAR image analysis, filtering, and interpretation. He has authored several tenths of research articles, textbooks, and computer software systems.

Waleed Ameen Al-Jawher: Dean of Engineering College, University of Isra, Jordan. He received a School of Research in Digital Signal Processing (2005). He received his Ph.D. in Digital Signal Processing from University of Wales University College of Swansea, United Kingdom (1986). He has a teaching experience in engineering for 32 years. A total of (15) National Awards. He Published over (224) papers, Supervised (202) M.Sc and PhD Students. He was the First professor Award of University of Baghdad, the First professor Award of the Ministry of Higher Education & Scientific Research of Iraq (National first Professor Award). His present areas of research interest are the field of DSP and Communication.

Atef Saleh Almashakbeh received his M.S. and Ph.D. degrees in electrical Engineering from Ukraine in 1997 and 2000, respectively. Dr. Almashakbeh is specialized in electrical and electronic machines. He conducted several researches in the field of induction motors, remote control, and case studies in electrical failures in machines. From 2001 to 2005, he worked as a faculty member at Albalqa Applied University in Jordan. Since 2005, Dr. Almashakbeh is an assistant professor at Tafila Technical University, Tafila- Jordan. His areas of research interest include DSP, wind energy, and medical machinery and apparatus. He has different research articles in these areas as well as some other secondary topics.

Ahed Ghodayyah was born in Amman in 1952. He received his B.Sc in applied physics from the University of Jordan in 1975, and his M.Sc in Electronic engineering from the University of Wails Institute of Science and Technology in UK in 1979. He is working as an instructor at Al Ahliyya Amman University. His areas of research interest are the fields of microprocessor systems and their applications in communications and DSP.